

Semi-Nonlinear Numerical 3D Time-Domain Simulation of a OWC Wave Power Plant

Christophe JOSSET, Gaëlle DUCLOS, Alain H. CLÉMENT

Laboratoire de Mécanique des Fluides (CNRS UMR6598)

Ecole Centrale de Nantes - FRANCE

ABSTRACT

The aim of this study is to develop a specific numerical method for the modelling of the free surface flow in and around a bottom standing three dimensional Oscillating Water Column (OWC) wave power plant. The inner nonlinear potential problem is solved using a Rankine time-domain BEM method, while the outer problem is posed as a linear time-domain and solved by a Kelvin BEM, using appropriate Green functions. The matching occurs on a fictitious vertical surface extending from the tip of the OWC front wall down to the sea bottom. Due to this coupling of nonlinear with linear solver, the method is called here a "semi-nonlinear" method. A general outline of the method is given here, together with preliminary results of a simplified implementation where both inner and outer solvers are linear.

INTRODUCTION

In this first application of the method, the power plant is supposed to be surrounded by an open ocean of constant water depth all around (fig.1). In other terms, the effects of local bathymetry and the presence of the coastline are not taken into account in the present study as it was in [4] which was a linear, frequency domain approach to the same problem. The goal here was to move from the previous frequency domain simulation to a time domain approach in order to model properly the observed nonlinear behavior of the free-surface flow inside the OWC water chamber, and to be able to incorporate in the future all the nonlinear terms describing the power take off and the air flow control system. It would not have been possible in a frequency domain approach. Due to the resonance of the water column, the nonlinearities are mainly concentrated inside the chamber, even in relatively calm wave climate outside. Then, the mixed approach consisting of solving the nonlinear problem inside and a linear one outside seemed in reasonable accordance with the physics, at least in a certain range of moderate wave climate. This is enforced by the fact that the geometry of the problem is very favorable to such a coupling. The coupling of nonlinear Rankine and linear Kelvin BEM methods has already been attempted for the modelling of the nonlinear flow around floating bodies ([10], [5],...), and it was often reported that numerical difficulties may arise at the matching point (line) of the three surfaces: the inner (moving) free surface, the fixed outer free-surface and the (locally) vertical matching boundary extending up the free-surface. Here, these three surfaces are never in contact with each other, but each one with the solid surface of the front wall. They are naturally separated, and the numerical problems are therefore avoided.

This study is divided into three parts. In the first one, a computer code (ACHIL3D - [9]) dedicated to the calculation of impulse response functions exerted on a floating body was modified to take the finite water depth into account; then the inner problem was formulated and solved in both, linear and nonlinear time domain approach. Finally, the coupling between inner and outer problems has been formulated, implemented, and tested. Preliminary results for linear/linear coupling are reported herein. Further results of

linear/nonlinear coupling will be presented during the Workshop.

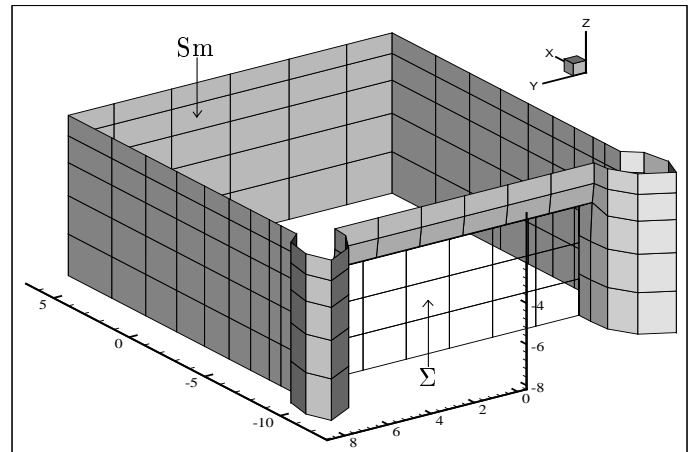


Fig.1 OWC power plant: the panelized boundary of the outer problem

THE OUTER LINEAR PROBLEM

The first step of this study consists in solving the outer linear problem of the OWC. The outer boundary of the plant can be divided into two parts (fig.1):

- 1) the external wall surface, S_m
- 2) the matching surface, Σ which represents the contact surface between inside and outside (transparent on the figure)

On each panel of Σ , the inner and the outer problems will be subsequently matched by enforcing the continuity of both potential and normal velocity (see section *coupling*). We will consider the outer potential $\Phi^e(M, t)$ as generated by the flux from the inner domain across Σ . It will be sought under the usual assumptions of irrotational potential flow

of incompressible and inviscid fluid, using the same zeroth order direct BEM method as exposed in [9]. The major difference here is that we use the finite depth, time-domain Green function $F_h(M, M', T)$, instead of the infinite depth operator. Then, before extending the program to the final OWC configuration as explained further, we have first validated this new option by computing the impulsive response of a vertical cylinder in finite depth due to of an horizontal motion. The results were successfully compared to McIver's analytical solution [6].

The Green function can be written in the generic form

$$F_h(M, M', T) = \delta(T)G_{0,h}(M, M') + H(T)G_h(M, M', T) \quad (1)$$

where $G_{0,h}(M, M')$ denotes the impulsive part of the function, and $G_h(M, M', T)$ the memory part. The third GREEN formula applied to both $\Phi^e(M, t)$ and $F_h(M, M', T)$ provides the necessary Fredholm-Volterra integral equation:

$$\begin{aligned} \frac{\Phi^e(M, T)}{2} - \iint_{S_{m+\Sigma}} \Phi^e(M', T) \frac{\partial G_{0,h}(M, M')}{\partial n'} dc \\ = - \iint_{S_{m+\Sigma}} G_{0,h}(M, M') \frac{\partial \Phi^e(M', T)}{\partial n'} dc + \\ \int_0^T d\tau \iint_{S_{m+\Sigma}} \left(\Phi^e(M', \tau) \frac{\partial G_h(M, M', T - \tau)}{\partial n'} \right. \\ \left. - G_h(M, M', T - \tau) \frac{\partial \Phi^e(M', \tau)}{\partial n'} \right) dc \end{aligned} \quad (2)$$

After discretization of equation (2), the external potential is then the single output of a linear process with the normal velocity on each panel as a multiple input. , we therefore solve for a set of eigen-problems, each of them corresponding to an impulsive normal velocity on one panel of Σ (say p_i for panel number i) and zero velocity on all the other panels of $\Sigma \cup S_m$. This is conceptually similar to the approach exposed by Bingham [12] at the 1998 issue of this Workshop series. The corresponding solution $\Phi_j^e(t)$, valid everywhere in the outer space will be denoted $\Phi_{i,j}^e(t)$ when expressed at the centroid of panel j . We then have, symbolically

$$\frac{\partial \Phi_{i,j}^e(t)}{\partial n} = \delta_{ij} \delta(t) \quad (3)$$

where δ_{ij} is the Kronecker symbol, and $\delta(t)$ the Dirac impulse distribution.

According to CUMMINS decomposition [11], this elementary solutions can be split into an impulsive and a memory part:

$$\Phi_{i,j}^e(t) = \delta(t) \Psi_{i,j} + H(t) \Phi_{i,j}^e(t) \quad (4)$$

So, after having solved all these eigen-problems, we are able to construct any potential on each facet for any kind of normal velocity history across the matching surface, by the following series of convolution integrals:

$$\Phi^e(i, t) = \sum_{j=1}^{n_\Sigma} \int_0^T \frac{\partial \Phi^e(j, t - \tau)}{\partial n} \cdot \Phi_{j,i}^e(\tau) d\tau \quad \forall i \in \Sigma \quad t \geq 0 \quad (5)$$

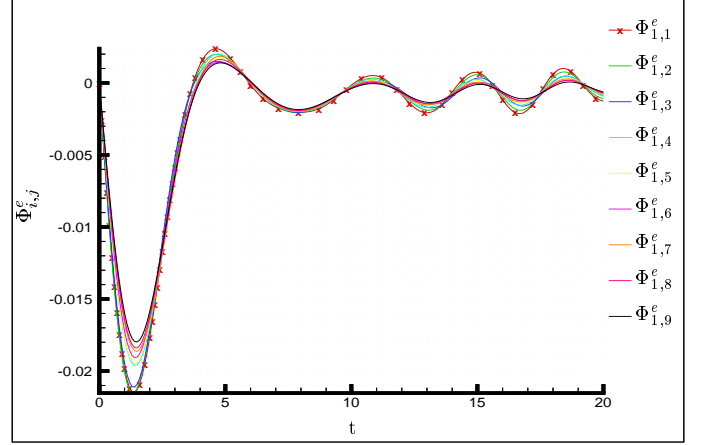


Fig.2 potential response on the matching boundary panels after an impulsive excitation in normal velocity

where n_Σ denotes the number of panels on the matching surface.

The global behavior of the solutions $\Phi_{j,i}^e(\tau)$ remains nearly same for all test cases (fig.2). Results are given here for the case where the excited facet is panel#1 (upper row, most external facet) when half the surface Σ is discretized into 9 panels. the table below shows the impulsive part $\Psi_{1,j}$, while memory functions $\Phi_{1,i}^e(\tau)$ are plotted on fig.2.

j	1	2	3
$\Psi_{1,j}$	-0.14E+00	-0.34E-01	-0.13E-01
4	5	6	7
-0.46E-01	-0.31E-01	-0.20E-01	-0.27E-01
8	9		
-0.24E-01	-0.20E-01		

We can notice that differences are more important on the impulsive part than on the memory part for this particular case.

evaluation of the GREEN function

The most important part of the cpu time in the solution of the outer problem is devoted to the evaluation of the Green function, which is far more difficult in finite than in infinite depth. We began using a routine based on [1] and [2] but this method was not sufficiently accurate for the calculation of the gradient of the function in the RHS of eq.2. So we finally turned to use a double Fourier transform of the frequency domain operators for $G_h(M, M', T)$; on the other hand, $G_{0,h}(M, M')$ was evaluated using Newman's expansion [7].

the diffraction problem

The diffraction problem is solved using basically the same code (ACHIL3D). The incident wave potential Φ_I is generated by an external spinning dipole [3], placed at some horizontal distance (typically 10 to 20 depth) in front of the OWC plant. The dipole, placed at mid-depth, start spinning at a given frequency from a state of rest a $t = 0$. The diffraction potential Φ_D on all the panels of the matching surface

Σ , computed by the Kelvin BEM method exposed above, is then stored for future simulations of the OWC when it is excited by external waves. For irregular incident wave fields, one can superimpose several spinning dipoles according to a given spectral discretization.

THE INNER PROBLEM

presentation

The next part of this study deals with the interior potential problem. The final goal is to couple the linear outer solution to the nonlinear solution of the inner problem. The intermediate stage which is now fully completed is to consider a linear problem also in the inner domain, but to solve it using a Rankine BEM method which will be extended later to account for interior free-surface displacement in time. The mesh of the inner domain is divided into three surfaces:

- 1) the interior wall surface , S_m
- 2) The coupling surface, Σ
- 2) The inner free-surface, S_l

formulation

The third Green formula applied to the unknown interior potential $\Phi^i(M, t)$ and to the Rankine source function $G_r(M, M')$ provides the integral interior problem formulation. A constant panel method was chosen here to remain consistent with the outer problem solver, avoiding problems on the matching surface.

$$\begin{aligned} \frac{\Phi^i(M, t)}{2} = & \iint_{S_m+S_l+\Sigma} \Phi^i(M', t) \frac{\partial G_r(M, M')}{\partial n'} dc \\ & - \iint_{S_m+S_l+\Sigma} G_r(M, M') \frac{\partial \Phi^i(M', t)}{\partial n'} dc \end{aligned} \quad (6)$$

A fourth order Runge-Kutta scheme was used to integrate the differential equations expressing the kinematic and dynamic free surface conditions; namely, at the present linear stage

$$\begin{cases} \eta = -\frac{\partial \Phi^i(M', t)}{\partial t} \\ \frac{\partial \eta}{\partial t} = \frac{\partial \Phi^i(M', t)}{\partial z} \end{cases} \quad M' \in S_l$$

On each panel of the boundaries, depending on the particular location, we have

	known	unknown
S_l	$\Phi^i(M, t)$	$\frac{\partial \Phi^i(M, T)}{\partial n}$
S_m	$\frac{\partial \Phi^i(M, T)}{\partial n}$	$\Phi^i(M, T)$
Σ	$\frac{\partial \Phi^i(M, T)}{\partial n}$ and $\Phi^i(M, T)$	

Before implementing the coupling with the outer problem in order to provide a closure to the above problem, we have tested our Rankine solver by imposing various kind of boundary condition on Σ . For each test, we have performed

a lot of checking related to energy and mass conservation in order to estimate the residual numerical dissipation of the code for several mesh size and different order of ODE solver.

The first straightforward test is to replace the matching surface by a solid wall, enforcing

$$\frac{\partial \Phi^i(M, T)}{\partial n} = 0 \quad M \in \Sigma$$

and releasing the fluid from a non-flat initial free-surface shape at $t = 0$. Figure 3 shows the evolution of potential and kinetic energy after such an experiment, where the internal free surface was given a half sine period shape. The balance between kinetic and potential energy is stable and nearly perfect (0.3% of energy loss on the reported simulation). An other test has consisted in imposing an artificial absorbing law on this surface ($S(i)$ is the area of the facet i), imposing a pressure proportional to the normal velocity on the panel, with a constant damping coefficient

$$\frac{\partial \Phi^i(M, T)}{\partial t} = -\frac{0.005}{S(i)} \frac{\partial \Phi^i(M, T)}{\partial n} \quad M \in \Sigma$$

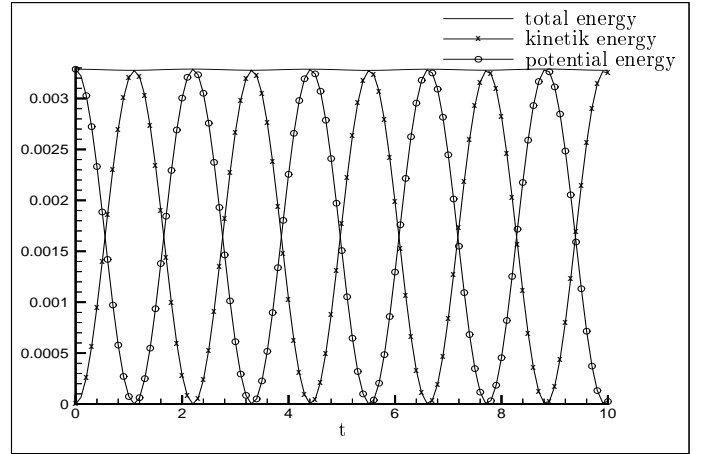


Fig.3 test of energy conservation of the inner solution after the release of the internal free-surface

The initial free-surface was uniformly surelevated in this test, simulating a non-zero initial pressure in the OWC chamber. Mass conservation has been checked by computing separately the integrated mass flux across the mean internal free-surface and the flux across the matching boundary Σ . Both curves are plotted on figure 4. The difference, which is here less than 0.1% confirms the quality of the simulation. A third order Runge-Kutta algorithm was sufficient to get energy and mas conservation reported here.

THE COUPLING METHOD

When the interior problem is coupled to the outer, the relation between the potential and the normal derivatives on Σ is provided by the solution of the linear outer problem, and by the matching conditions

$$\begin{aligned} \Phi^e(M, t) = & \Phi^i(M, t) \\ \frac{\partial \Phi^e(M, T)}{\partial n} = & -\frac{\partial \Phi^e(M, T)}{\partial n} \quad \forall M \in \Sigma; t \geq 0 \end{aligned}$$

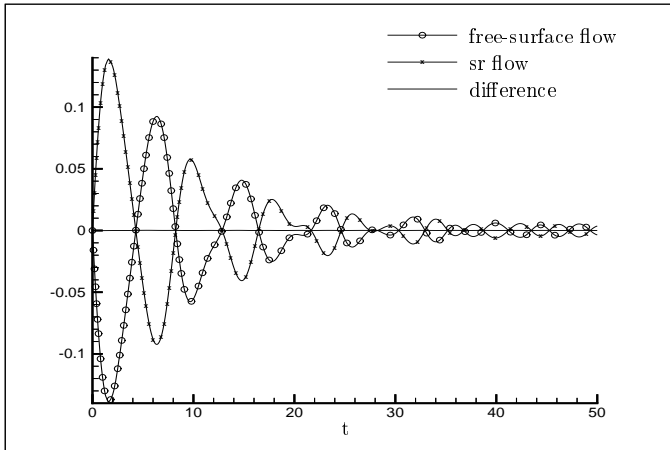


Fig.4 flow across the inner free-surface and the matching boundary after the release of an initial pressure step above the internal free-surface

Such a matching between nonlinear inner solution and linear outer solution in time domain simulations was used by e.g Dommermuth and Yue [10], and Hamilton and Yeung [5] with the so-called *shell-function* method. Replacing $\Phi^e(M, t)$ by $\Phi^i(M, t)$ and idem with their derivatives in eq.5 provides the necessary system to eliminate $\Phi^i(k, t)$ in the RHS of the integral equation eq.6. The forcing term of the inner problem now contains convolution integrals which represent the influence of the history of the external flow on the internal problem. It contains also the terms representing the influence on each panel of the incident and diffracted wave potentials supplied independently (and possibly in advance) by the outer linear BEM.

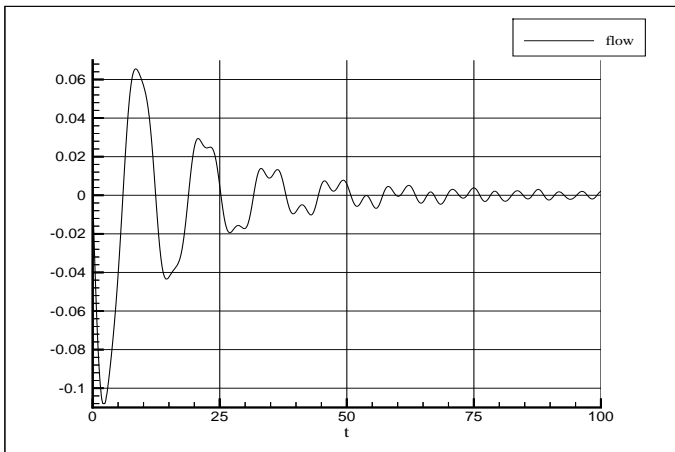


Fig.5 impulse response function of the pressure radiation problem for an isolated bottom standing OWC

The first application reported here (fig.5) is related to the linear response of the OWC of fig.1 to a step of pressure (equivalent to $0.2h$ in water column units). Again the total free-surface flow is plotted on fig.5. It compares very closely to the impulse response function of the same OWC plant

geometry computed by Fourier transform of the frequency domain approach in [4] (see fig9 p.151).

This comparison has made us confident in our implementation of the coupling method, and open the way to the continuation of the study towards the linear/nonlinear coupling which is now being implemented and tested.

REFERENCES

- [1] CLÉMENT, A.H., MAS, S. Computation of the finite water depth time domain Green function in the small time range . Proc. 9th Int. Workshop on Water Waves and Floating Bodies; Kuju, Japon, pp49/53.(1994)
- [2] MAS, S., CLÉMENT, A.H. Computation of the Finite Depth Time-Domain Green Function in the Large Time Range. Proc. 10th Int. Workshop on Water Waves and Floating Bodies ; Oxford, pp 165/169.(1995)
- [3] CLÉMENT, A.H. The Spinning Dipole : an Efficient Unsymmetrical Numerical Wavemaker; Proc. 14th Int. Workshop on Water Waves and Floating Bodies ; Port Huron, Michigan, pp.29-32.(1999)
- [4] BRITO-MELO, A., HOFMANN, T., SARMENTO, A.J.N.A., CLÉMENT, A.H., DELHOMMEAU, G. Numerical Modelling of OWC-Shoreline Devices Including the Effects of Surrounding Coastline and Non-flat Bottom ; *Int Journal of Offshore and Polar Engineering*, Vol11, n°2, pp.147-154.(2001)
- [5] HAMILTON, J.A., YEUNG, R.W. Shell-Function Solutions or Three-Dimensional Nonlinear Body-Motion Problems ;*Ship Technology Research*, Vol44, n°2, pp.62-70.(1997)
- [6] MCIVER, P. ,Transient Fluid Motion Due to the Forced Horizontal Oscillations of a Vertical Cylinder ;*Applied Ocean Research*, Vol16, n°2, pp.347-351.(1994)
- [7] NEWMAN, J.N. The Approximation of Free-Surface Green Functions ;*Wave Asymptotics*, Vol16, n°2, pp.107-135 .(1994)
- [8] WEHAUSEN J.V., LAITONE E.V. Surface Waves ;*Encyclopedia of Physics, Fluids Dynamics III*, Vol3, n°2, pp.446-778 .(1994)
- [9] CLÉMENT, A.H. Using differential properties of the Green function in seakeeping computational codes . Proc. 7th Int. Conf. Numerical Ship Hydrodynamics ; Nantes, France, pp6,5-1,5-15.(1999)
- [10] DOMMERMUTH D.G.,YUE D.K.P. Numerical simulations of nonlinear axisymmetric flows with a free surface ;*Journal of Fluid Mechanics*, Vol178,° pp.195-219.(1987)
- [11] CUMMINS W., E., (1962) The impulse response functions and ship motions. *Schiffstechnik*, Vol9, pp.101-109.
- [12] BINGHAM, H.B. (1998) Computing The Green Function for linear wave-body interaction, in Proc. 13th Int. Workshop Water Waves and Floating Bodies, Alphen ann den Rijn, pp.5-8.

Discussion Sheet

Abstract Title :	Semi-nonlinear numerical 3D time-domain simulation of a OWC wave power plant		
(Or) Proceedings Paper No. :	16	Page :	061
First Author :	Josset, C., Duclos, G. and Clément, A.H.		
Discussor :	Rod C.T. Rainey		
Questions / Comments :			
<p>Of the Oscillating water column (OWC) principle generally, I would say from an engineering point of view that “C’est magnifique, mais ce n’est pas la guerre”. Its power-to-weight ratio is too low for it ever to be economic. It is not in the same league as the floating wave power device described in my paper at the last workshop, and featured on the cover of these Proceedings.</p>			
Author’s Reply :			
<i>(If Available)</i>			
Author did not respond.			

Discussion Sheet

Abstract Title :	Semi-nonlinear numerical 3D time-domain simulation of a OWC wave power plant		
(Or) Proceedings Paper No. :	16	Page :	061
First Author :	Josset, C., Duclos, G. and Clément, A.H.		
Discussor :	Ronald W. Yeung		
Questions / Comments :			
<p>The treatment of the outer problem uses the "shell-function method" introduced in my 1985 paper in the IUTAM Symposium on Ocean Wave Energy Extraction organized by David Evans. It is gratifying to see this can be applied to a wave-energy project of complex geometry. It is a powerful formulation to treat time-dependent problems.</p>			
Author's Reply :			
<i>(If Available)</i>			
Author did not respond.			

Questions from the floor included; Paul Sclavounos & Fritz Ursell.